SCIENTIFIC REPORTS

OPEN

Characterization of donor and recipient CD8+ tissue-resident memory T cells in transplant nephrectomies

Received: 23 November 2018
Accepted: 29 March 2019
Published online: 12 April 2019

Kitty de Leur[1,2], Marjolein Dieterich[1], Dennis A. Hesselink[1], Odilia B. J. Corneth[3], Frank J. M. F. Dor[2], Gretchen N. de Graav[1], Annemiek M. A. Peeters[1], Arend Mulder[5], Hendrikus J. A. N. Kimenai[2], Frans H. J. Claas[5], Marian C. Clahsen-van Groningen[4], Luc J. W. van der Laan[2], Rudi W. Hendriks[3] & Carla C. Baan[1]

Tissue-resident memory T (T_{RM}) cells are characterized by their surface expression of CD69 and can be subdivided in CD103+ and CD103− T_{RM} cells. The origin and functional characteristics of T_{RM} cells in the renal allograft are largely unknown. To determine these features we studied T_{RM} cells in transplant nephrectomies. T_{RM} cells with a CD103+ and CD103− phenotype were present in all samples ($n = 13$) and were mainly CD8+ T cells. Of note, donor-derived T_{RM} cells were only detectable in renal allografts that failed in the first month after transplantation. Grafts, which failed later, mainly contained recipient derived T_{RM} cells. The gene expression profiles of the recipient derived CD8+ T_{RM} cells were studied in more detail and showed a previously described signature of tissue residence within both CD103+ and CD103− T_{RM} cells. All CD8+ T_{RM} cells had strong effector abilities through the production of IFNγ and TNFα, and harboured high levels of intracellular granzyme B and low levels of perforin. In conclusion, our results demonstrate that donor and recipient T_{RM} cells reside in the rejected renal allograft. Over time, the donor-derived T_{RM} cells are replaced by recipient T_{RM} cells which have features that enables these cells to aggressively respond to the allograft.

Over the last two decades, the presence and importance of a non-migrating subset of memory T cells surveying immune responses in non-lymphoid tissues has been recognized: the so-called tissue-resident memory T (T_{RM}) cells[1,2]. Their restricted anatomical localization in combination with their effector memory phenotype enables T_{RM} cells to rapidly respond to local antigens. Today, two distinct subsets of T_{RM} cells have been identified: CD69+CD103+ and CD69+CD103− T_{RM} cells (hereafter referred to as CD103+ T_{RM} cells and CD103− T_{RM} cells, respectively)[3–6]. CD69 is a C-type lectin that was originally identified as a marker of activated T cells but is also involved in tissue retention of T_{RM} cells[2,7–9]. CD69 binds to and down-regulates the G protein-coupled receptor sphingosine 1 phosphate (S1PR1) expressed on the T cell membrane, resulting in a decreased ability of T_{RM} cells to sense the S1P gradient that promotes migration of memory T cells from the blood into peripheral tissue[7–9]. A unique T_{RM} cell gene expression profile has recently been identified by Kumar *et al.* with 31 core genes that are differentially up- or downregulated in CD69+ T_{RM} cells isolated from human lung and spleen[10]. The other recognized T_{RM} marker, CD103, is an αE integrin that binds E-cadherin which is expressed on epithelial tissues[11]. Today, no clear consensus exists about the functional differences between CD103+ and CD103− T_{RM} cells.

Although the presence and antigen specificity of T_{RM} cells is recognized in several non-lymphoid human tissues (*e.g.* skin, liver, lungs, intestine and brain), the presence and function of T_{RM} cells in the human kidney is currently unknown[4,5,12–16]. In experimental mouse models, it was demonstrated that T_{RM} cells homed to the

[1]Department of Internal Medicine, Division of Nephrology and Transplantation, Erasmus MC, University Medical Center Rotterdam, Rotterdam, The Netherlands. [2]Department of Surgery, Division of HPB & Transplant Surgery, Erasmus MC, University Medical Center Rotterdam, Rotterdam, The Netherlands. [3]Department of Pulmonary Medicine, Erasmus MC, University Medical Center Rotterdam, Rotterdam, The Netherlands. [4]Department of Pathology, Erasmus MC, University Medical Center Rotterdam, Rotterdam, The Netherlands. [5]Department of Immunohematology and Blood Transfusion, Leiden University Medical Center, Leiden, The Netherlands. Correspondence and requests for materials should be addressed to K.d.L. (email: k.deleur.1@erasmusmc.nl)

	Recipient				Transplantation						
	Gender	Age at nephrectomy (y)	Cause of ESRD	Number of previous renal transplants	Donor type	CMV status donor*	CMV status acceptor*	Maintenance IS	Anti-rejection treatment	Time to explantation (days)	Cause of graft failure
1.	M	30	Hypertensive nephropathy	0	L	−	+	Tac, MMF, Pred	MP, IvIg, plasmaferese, Alemtuzumab	8	aTCMR2B and aABMR and pyelonephritis
2.	F	48	ADPKD	0	L	−	+	Bela, Tac**, MMF, Pred, Basiliximab	MP, Alemtuzumab	12	aTCMR2B and aABMR
3.	M	63	Hypertension nephropathy	0	D	+	+	Tac, MMF, Pred, Basiliximab	MP, IVIg	15	aTCMR 2B and aABMR
4.	F	28	GPA	1	L	+	−	Tac, MMF, Pred	IVIg, Alemtuzumab	150	aTCMR3 and aABMR
5.	M	46	ADPKD	0	L	+	−	Tac, MMF, Pred	MP	270	aTCMR3
6.	F	67	Hypertension nephropathy	0	D	−	+	None#	MP	390	aTCMR3 and aABMR
7.	M	71	Diabetic nephropathy	1	D	+	+	Tac, MMF	MP	2268	aTCMR3 and c-aABMR
8.	M	29	HUS	0	D	−	−	Tac, MMF	None	2340	c-aABMR
9.	M	24	FSGS	0	L	+	+	MMF, Pred, Ecu***	MP, IVIg	2520	c-aABMR
10.	M	51	Congenital hydronephrosis	0	D	−	−	Tac	None	3240	aTCMR2B and aABMR
11.	F	51	poststreptococcal glomerulo-nephritis	0	D	+	−	None#	None	3780	c-aABMR and c-aTCMR
12.	M	53	Hypertension nephropathy	1	L	+	+	Tac, Pred	None	4320	aTCMR3
13.	M	57	Hypertension nephropathy	0	D	+	+	Aza, Pred	None	9360	End-stage kidney

Table 1. Patient baseline characteristics. *CMV status prior to transplantation. **Switch from Belatacept to Tacrolimus due to rejection. ***No tacrolimus due to thrombotic microangiopathy. #Decreased IS and restarted dialysis. aABMR = acute antibody mediated rejection; ADPKD = autosomal dominant polycystic kidney disease; aTCMR = acute T cell-mediated rejection; Aza = azathioprine; CMV = cytomegalovirus; D = deceased; Ecu = eculizumab; ESRD = end-stage renal disease; FSGS = focal segmental glomerulosclerosis; GPA = granulomatosis with polyangitis; HUS = hemolytic uremic syndrome; IS = immunosuppression; IVIg = intravenous immunoglobulin; L = living; MP = methylprednisolone; MMF = mycophenolate mofetil; Pred = prednisone; Tac = tacrolimus.

kidney where they resided, and that this migration was promoted by TGF-β[17,18]. Otherwise, little is known about the functional properties of these kidney T_{RM} cells[19].

Transplantation of a renal allograft is accompanied by the transfer of donor leucocytes. It is probable that these leucocytes also include donor-derived T_{RM} cells. It is, however, unknown if these cells persist after transplantation or whether they are replaced by T_{RM} cells of recipient origin. It is therefore informative to identify the donor or acceptor origin of these cells and thus the degree of chimerism. This will help us to understand if donor T_{RM} cells are present in the allograft to control local viral and bacterial responses[20] and whether these T_{RM} cells might be enriched for graft-*versus*-host (GvH) reactive clones, as seen in intestinal transplant patients[21–23]. The presence of recipient T_{RM} cells will shed light on their potential role in alloreactivity and will show if recipient T cells differentiate into T_{RM} cells in the renal allograft.

Here, we postulate that T_{RM} cells are present in the renal allograft and that these cells are primarily from recipient origin and are capable of mounting an allo-reactive response. To this end, we used the unique tissue resource of transplant nephrectomies from immunosuppressed patients to study the presence, provenance (donor or recipient), and the effector phenotype of CD103+ T_{RM} cells (CD69+CD103+), CD103− T_{RM} cells (CD69+CD103−), and recirculating T cells not expressing the tissue retention markers CD69 and CD103 (CD69−CD103−). We performed similar control experiments with spleen cells of organ donors, a lymphoid cell population in which T_{RM} cells are known to be present[3,10].

Results

T cells of donor and recipient origin are present in the renal allograft. Thirteen transplant nephrectomy specimens were studied. Patient demographics are listed in Table 1. These kidney allografts failed either acute ($n = 4$) or chronically ($n = 9$) as a result of humoral, cellular or mixed-type rejection and were removed after a mean time of 6.1 years (range: 8 days–26 years).

After the isolation procedure, CD3+ T cells were detected in all renal allografts with a median proportion among the total viable lymphocytes of 72.1% (range: 30.1–78.5%; Fig. 1A). Of the CD3+ T cells, 37.6%

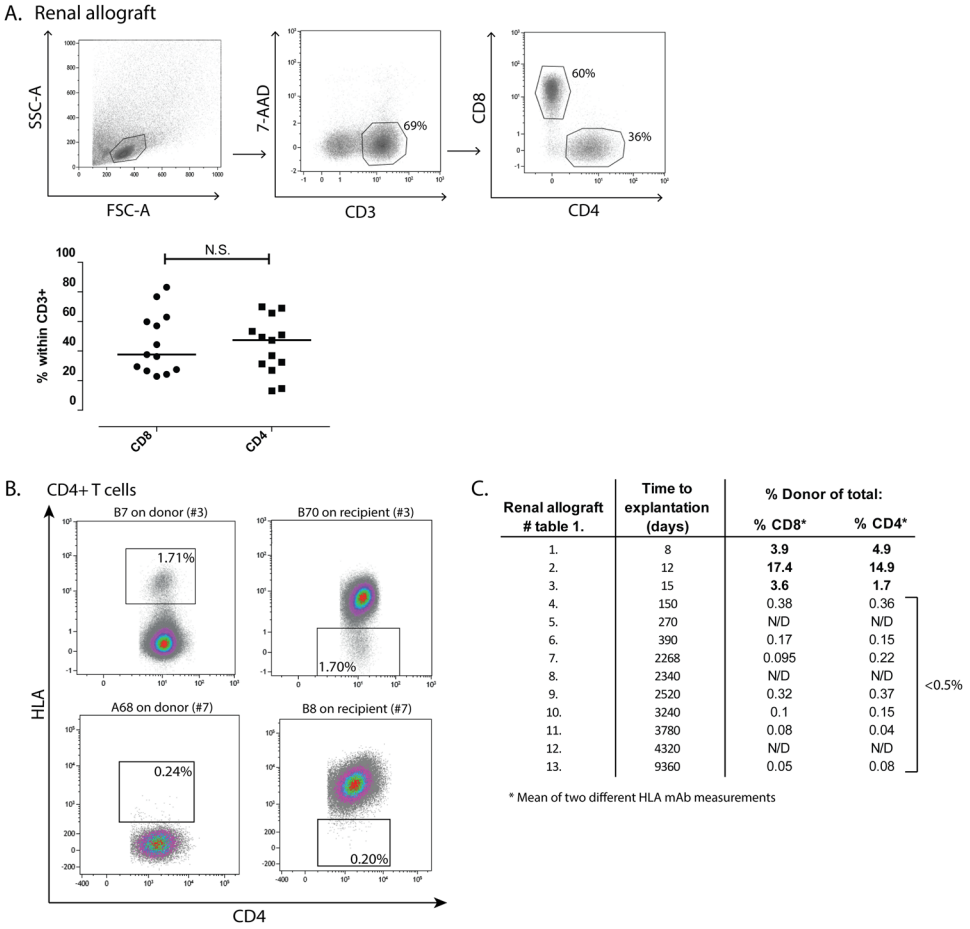

C.

Renal allograft # table 1.	Time to explantation (days)	% Donor of total: % CD8*	% CD4*	
1.	8	**3.9**	**4.9**	
2.	12	**17.4**	**14.9**	
3.	15	**3.6**	**1.7**	
4.	150	0.38	0.36	
5.	270	N/D	N/D	
6.	390	0.17	0.15	
7.	2268	0.095	0.22	
8.	2340	N/D	N/D	<0.5%
9.	2520	0.32	0.37	
10.	3240	0.1	0.15	
11.	3780	0.08	0.04	
12.	4320	N/D	N/D	
13.	9360	0.05	0.08	

* Mean of two different HLA mAb measurements

Figure 1. CD8+ and CD4+ T cells of donor and recipient origin are present in the renal allograft. Lymphocytes were isolated from the rejected renal allografts and subsequently stained and analysed by flow cytometry. (**A**) Gating strategy used to detect CD3+ T cells within the total viable lymphocytes, of which the CD8+ and CD4+ T cells were selected. (**B**) Typical examples of renal lymphocyte samples of patient number three and seven stained with mAb against human leukocyte antigen (HLA) class I antigens within the CD4+ T cells. Proportions of cells originating from the donor are depicted. (**C**) Table with numbers referring to the renal allografts described in Table 1, the time to explantation in days, and the proportions of donor cells detected within the CD8+ and CD4+ T cell compartment. Frequencies of the cells are presented as individual proportions with medians. HLA = human leukocyte antigen; N.S. = not significant; N/D = not determined.

(22.9–83.2%) were CD8+ and 47.4% (13.1–70.0%) were CD4+ T cells (Fig. 1A). The CD3+ T cells isolated from nephrectomy number three and four (Table 1) were capable of mounting an allogeneic response, since both the proportions of proliferating cells and the expression of the degranulation marker CD107a increased in the presence of donor antigen, while a negligible response was measured after stimulation with irradiated recipient PBMCs (Supp. Fig. 1A,B). In addition, the cells of patient number three reacted to a fully HLA mismatched 3rd party and responded to donor antigen by the production of IFNγ (Supp. Fig. 1A–C).

Next, the degree of chimerism was studied in the explanted renal allografts. Conjugated HLA-mAbs were available to distinguish recipient from donor cells in ten renal lymphocyte samples. In the example depicted in Fig. 1B (upper panel), the proportions of donor cells measured by a mAb against HLA-B7 (donor positive) and a mAb against HLA-B70 (acceptor positive) resulted in similar donor proportions of 1.71% and 1.70% respectively, showing chimerism in this sample. Three out of the ten renal allografts studied were removed within the first month after transplantation (Table 1). In these renal allografts, clear populations of CD4+ and CD8+ T cells from donor origin were detected (Fig. 1C). The renal allografts removed five months or later after transplantation only contained marginal proportions (<0.5%) of donor-derived T cells, and we could not distinguish a clear positive and negative fraction in these samples as depicted in the dot plots of patient number 7 in Fig. 1B (lower panel). Thus, high proportions of donor-derived T cells were only seen in early rejection nephrectomies.

T_{RM} cells are present in the renal allograft. The absence of T_{RM} cells in PBMC fractions and the presence of T_{RM} cells in the spleen was recognized in previous studies[3,10]. Subsequently we used PBMCs from healthy controls as a negative control and splenocytes of deceased organ donors as a positive control for T_{RM} cell identification. CD69+ T_{RM} cells were present in all transplant nephrectomy specimens with a median proportion of

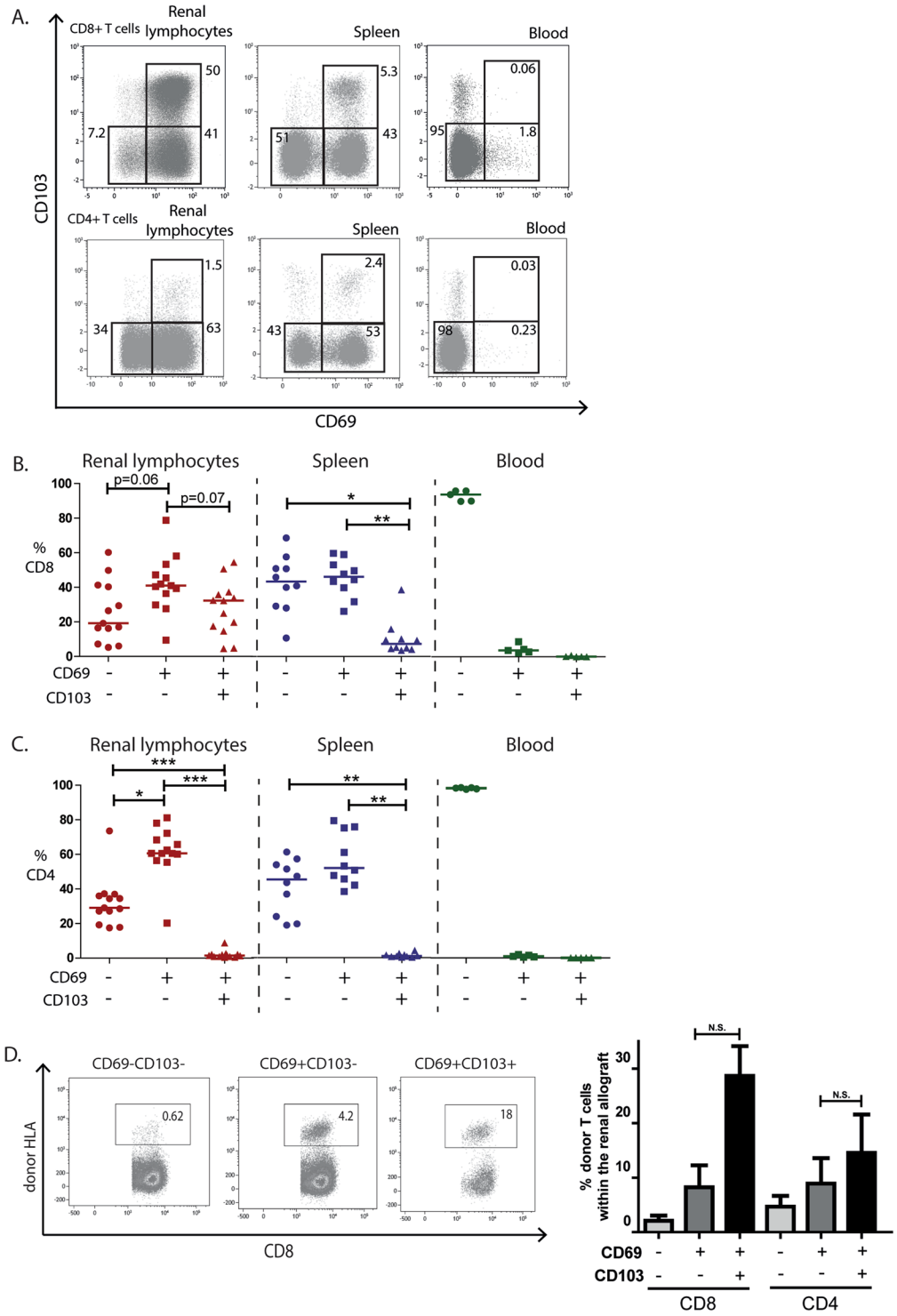

Figure 2. T_{RM} cells are present within CD8+ and CD4+ T cells in the renal allograft. Lymphocytes from rejected renal allografts, spleens of organ donors, and blood from healthy individuals were stained with mAb against CD69 and CD103. (**A**) Representative examples of the gating strategy of CD69 and CD103 of lymphocytes originating from the renal allograft, spleen, and blood. Proportions of the gated areas are depicted within the dot-plots. (**B**,**C**) Quantified data of the recirculating T cells (CD69−CD103−), CD103− T_{RM} cells (CD69+CD103−), and CD103+ T_{RM} cells (CD69+CD103+) subsets within the CD8+ T cell compartment (**B**) and CD4+ T cell compartment (**C**) of the renal allograft, spleen, and blood (blood $n = 5$, spleen $n = 10$, renal allograft $n = 13$). Frequencies of the cells are presented as individual proportions with medians. Significant differences were calculated and presented (*$p < 0.05$, **$p < 0.01$, ***$p < 0.001$). (**D**) mAb against HLA class I antigens were used to discriminate between donor and recipient lymphocytes. Typical example dot plots and quantified data of proportions of donor-derived cells within the CD103+ T_{RM} cells, CD103− T_{RM} cells

and recirculating T cells are depicted of the transplant nephrectomies removed within the first month after transplantation (Table 1, patient 1 to 3). Frequencies of the positive cells are depicted within the dot plots. Frequencies of positive cells are shown as mean with the SEM ($n = 3$; N.S. = not significant).

73.2% in the CD8+ T cell compartment and 62% in the CD4+ T cell compartment (Fig. 2A). We subdivided the T_{RM} cells in CD103+ T_{RM} (CD69+CD103+) cells and CD103− T_{RM} cells (CD69+CD103−). The median proportion of CD103+ T_{RM} cells within the CD8+ T cell compartment was 32.3% (range: 4.5–54.4%) compared to 1.4% (0.7–8.8%) within the CD4+ T cell compartment. In contrast, CD103− T_{RM} cells were more evenly distributed among the CD8+ (40.9%, 9.4–78.8%) and CD4+ (60.6%, 20.2–81.2%) T cell compartments (Fig. 2B,C). As expected, minimal proportions of CD103+ T_{RM} cells and CD103− T_{RM} cells were found in peripheral blood, while both T_{RM} cell subsets were present in the spleen (Fig. 2). Similar proportions of CD4+ and CD8+ T_{RM} cells were detected in two native kidneys that were discarded for transplantation (Supp. Fig. 2). No significant differences were detected when we subdivided the CD103+ and CD103− T_{RM} cells of the transplant nephrectomies based on donor type, Banff 2017 category and time to explantation (Supp. Fig. 3A–C). Of interest might be the observation that in chronic-active antibody-mediated rejection (c-aABMR) specimens the proportion of CD103− T_{RM} cells was low (Supp. Fig. 3B). However, this observation is only based on two c-aABMR cases.

We questioned whether T_{RM} cells of donor or recipient origin were present in the kidneys explanted in the first month after transplantation (Fig. 1C). For that we stained the renal lymphocytes of the transplant nephrectomies removed within the first month after transplantation (patients 1–3, Table 1) again with antibodies recognizing either donor or recipient HLA molecules. Remarkably, donor-derived lymphocytes were most prominent within the CD103+ T_{RM} cell population, with lower levels of donor cells in the CD103− T_{RM} cells and recirculating T cell compartments (Fig. 2D). This was observed for both CD8+ and CD4+ donor T cells. These data suggest the increased ability of donor-derived CD103+ T_{RM} cells to reside in the renal allograft compared to the remaining donor-derived T cells.

Because the proportion of CD103+ T_{RM} cells was very low among the CD4+ T cells, not allowing further analysis, we focused on the CD8+ T_{RM} cells for subsequent experiments. In addition, the three renal allografts explanted within the first month after transplantation were excluded in order to study a pure population of recipient T_{RM} cells that may mediate and control the local immune response.

Expression of T_{RM} signature genes. To define the gene expression profile of the T_{RM} cells, we selected 8 genes from a set of signature genes described by Kumar *et al.* that are differentially expressed between CD69− and CD69+CD8+ T cells isolated from the spleen and lung[10]. We compared the expression of these genes in cells isolated form the renal allograft and in splenocytes in the following FACS-sorted CD8+ T cell populations: CD69+CD103+ T_{RM} cells, CD69+CD103− T_{RM} cells, and CD69−CD103− (recirculating) T cells. The gating strategy for the FACS sort experiments is depicted in Fig. 3A.

We used RT-qPCR to quantify the expression of genes that are involved in pathways that mainly control T cell migration, adhesion and activation. Separate heat maps were created of the gene expression levels of the renal allograft and spleen (Fig. 3B). Overall, two clusters were identified in the heat maps of both the renal allograft and spleen: a cluster of genes upregulated in the total T_{RM} cells (CD103+ and CD103− T_{RM} cells) and a cluster of genes downregulated in the total T_{RM} cells, compared to the recirculating T cells (Fig. 3B). The gene expression levels of the adhesion marker ITGA1 (CD49a) were especially high in the CD103+ T_{RM} cells, with lower expression levels in the CD103− T_{RM} cells and recirculating T cells. Chemokine receptor CXCR6 and cytokine IL-10 were clearly expressed at a higher level in the total T_{RM} cell subsets compared to the recirculating T cells. In both the spleen and renal allograft samples, the T cell trafficking and homing markers S1PR1, Kruppel-like transcription factor 2 (KLF2), SELL (CD62L), KLF3 and CX3CR1 were expressed at a lower level in the total T_{RM} cells compared to the expression levels in the recirculating T cells. When we clustered the FACS-sorted samples of the renal allograft and spleen, the CD103+ T_{RM} cells and CD103− T_{RM} cells clearly clustered together as opposed to the recirculating T cells (Supp. Fig. 4). In summary, the total population of T_{RM} cells can be clearly distinguished from the recirculating T cells based on their gene expression profile. In addition, similar gene expression levels were found in the different T cell subsets when comparing the renal allograft and the spleen samples.

T_{RM} cells in the renal allograft have an effector memory phenotype. To demonstrate that the CD8+ T_{RM} cells found in the renal allograft have an effector phenotype we stained the cells for the surface molecules CCR7 and CD45RO. With these markers naïve (CCR7+CD45RO−), central memory (CM, CCR7+CD45RO+), effector memory (EM, CCR7−CD45RO+) and highly-differentiated effector memory (EMRA, CCR7−CD45RO−) T cells were discriminated (see Fig. 4A for a typical example). While the recirculating T cells in the renal allograft and spleen were more divergent in terms of CCR7 and CD45RO expression, the majority of the CD103− T_{RM} cells and CD103+ T_{RM} cells were CCR7−CD45RO+ and thus EM T cells (Fig. 4B). This finding is in line with previous studies in non-lymphoid tissues where the majority of T_{RM} cells was also of an EM phenotype[3,10].

T_{RM} cells are capable of producing effector molecules. The capacity of the cells to produce the pro-inflammatory cytokines IFNγ and TNFα was measured after polyclonal stimulation. No change in the expression and proportion of CD69+ cells before and after three hours of polyclonal T cell stimulation was observed, in contrast to an altered expression of CD69 and CD103 on the CD8+ T cells after seven days allostimulation (Supp. Figs 5 and 6). Subsequently, we compared the T_{RM} cell subsets and the recirculating T cells after stimulation for their cytokine production capacity.

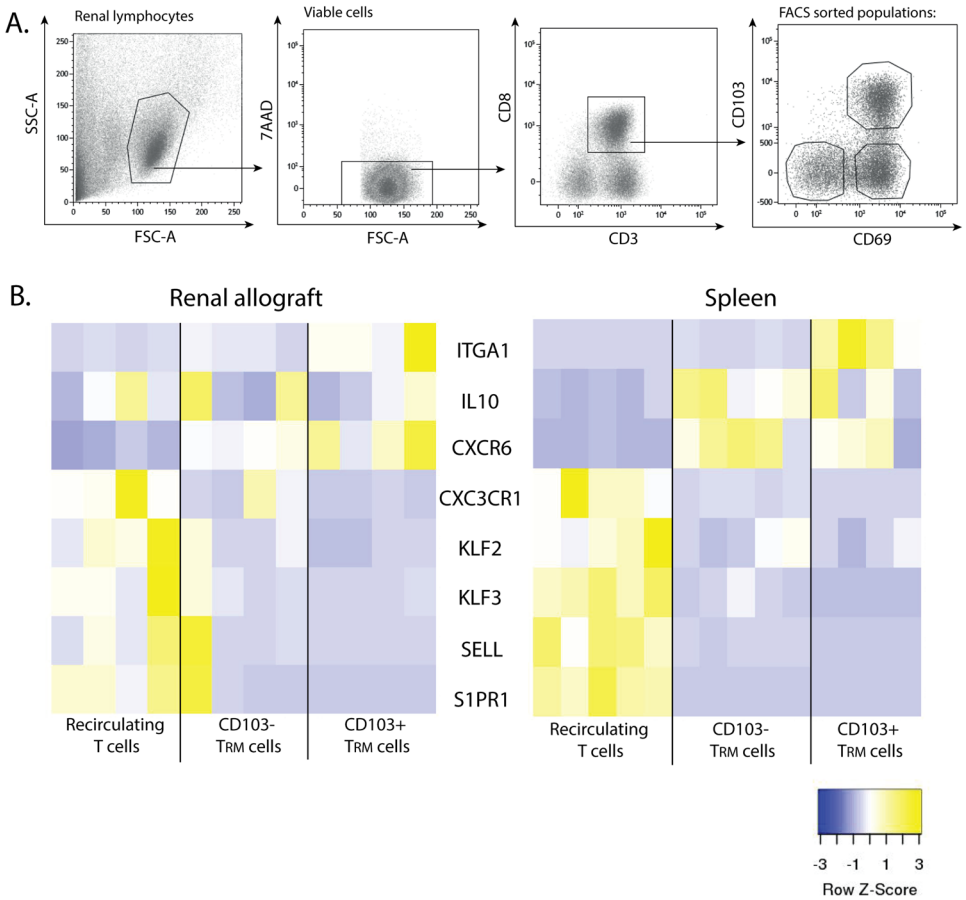

Figure 3. Expression of T_{RM} signature genes. (**A**) Typical example of the gating strategy used after fluorescence activated CD8+ cell sorting to obtain recirculating T cells (CD69−CD103−), CD103− T_{RM} cells (CD69+CD103−), and CD103+ T_{RM} cells (CD69+CD103+). Cells were gated by forward- and side-scatter followed by 7-AAD negative (viable) gating. (**B**) Heatmaps depicting the normalized gene expression of eight signature genes known to be upregulated (yellow) or downregulated (blue) in T_{RM} cells of the renal allograft and spleen. Spleen $n = 5$, renal lymphocytes $n = 4$.

After stimulation, all resident and recirculating CD8+ T cell subsets expressed high levels of IFNγ (Fig. 5A). A slightly higher expression in the IFNγ production capacity was observed in the CD103+ T_{RM} cells in both renal allograft and spleen compared to the recirculating and CD103− T_{RM} cell subsets (Fig. 5A). For TNFα, a different profile was found with the highest expression levels in the recirculating T cells, lower levels in the CD103− T_{RM} cells and the lowest levels in the CD103+ T_{RM} cells (Fig. 5B). Within the spleen, the differences in TNFα proportions were significantly different between the different subsets (Fig. 5B). Highly effector CD8+ T cells that were concurrently positive for IFNγ and TNFα were present in both the renal CD103− and CD103+ T_{RM} cells (Supp. Fig. 7).

To determine the degranulation capacity of the different CD8+ T_{RM} cell subsets, intracellular granzyme B and perforin expression were measured (Fig. 5C,D). In the renal allograft, the intracellular granzyme B levels did not significantly differ between the recirculating T cells, the CD103− T_{RM} cells and CD103+ T_{RM} cells (Fig. 5C). The granzyme B levels within the spleen were significantly lower in the CD103+ T_{RM} cells compared to both the recirculating T cells and the CD103− T_{RM} cells. With regard to the intracellular levels of perforin, the same trend between the different subsets was found in the renal allograft samples compared to the spleen samples (Fig. 5D). The perforin levels were significantly lower in the CD103+ T_{RM} cells compared to the recirculating T cells (Fig. 5D). Together, these data show that T_{RM} cells, but also the recirculating T cells, are capable of mounting and effector response.

Discussion

In this study, we demonstrate that (1) T cells with a resident memory phenotype and gene expression profile are present in the renal allograft, (2) T_{RM} cells in the renal allograft have strong immunostimulatory capacity, and (3) the donor-derived cells present are mainly CD103+ T_{RM} cells and are replaced by recipient-derived T cells within five months after transplantation. An overview of these findings is depicted in Fig. 6.

No major differences were found in gene expression signature and functional profiles between the CD103+ T_{RM} and CD103− T_{RM} cells, highlighting that these two T_{RM} cell subtypes have comparable characteristics.

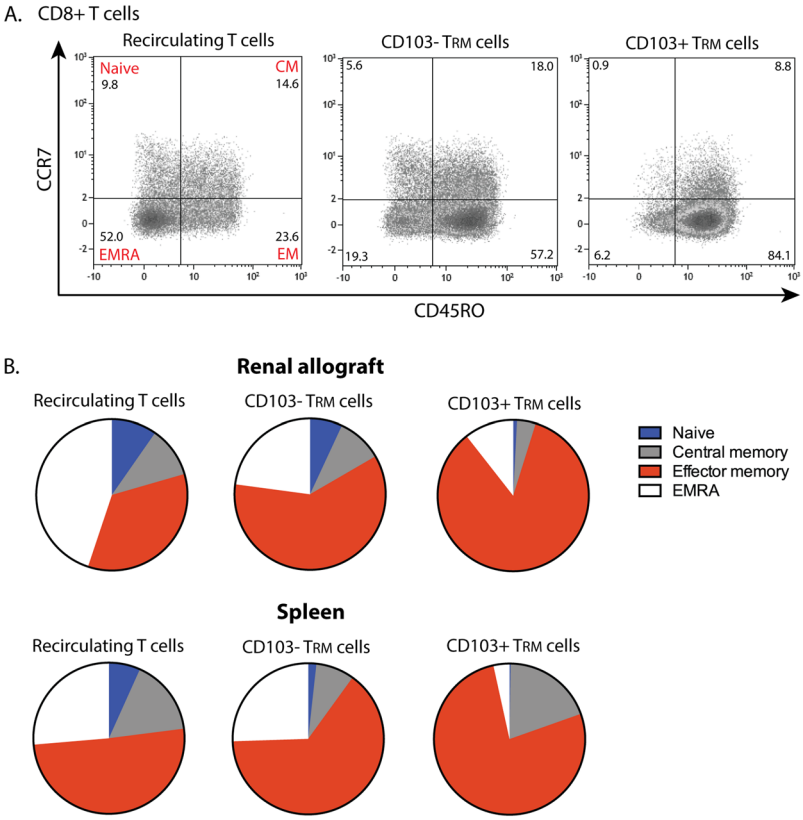

Figure 4. T_{RM} cells in the renal allograft have an effector memory phenotype. (**A**) Typical examples of dot plots presenting the distribution of naïve T cells (CCR7+CD45RO−), central memory T cells (CM; CCR7+CD45RO+), effector memory T cells (EM; CCR7−CD45RO+), and EMRA T cells (CCR7−CD45RO−) within the CD8+ recirculating T cells, CD103− T_{RM} cells and CD103+ T_{RM} cells of the renal allograft. Numbers within the dot plots indicate proportions of the different cell subsets. (**B**) Pie charts representing the median proportion of naïve, central memory, effector memory, and EMRA T cells within the CD8+ recirculating T cells, CD103− T_{RM} cells and CD103+ T_{RM} cells of the renal allograft and spleen (renal lymphocytes $n = 6$, spleen $n = 8$).

Previous studies report that CD103+ T_{RM} cells reside more predominantly within the barrier tissues while CD103− T_{RM} cells are more common within non-barrier tissues[18]. In transplantation, CD8+CD69−CD103+ T cells are involved in the effector mechanism of chronic and acute renal allograft rejection[24–27]. In addition, in urinary samples, the mRNA levels of CD103 predicted acute renal allograft rejection[28]. However, in the context of kidney transplantation the exact difference in CD103+ and CD103− T_{RM} cells is unknown and of interest for further analysis.

The majority of the T_{RM} cells detected in the renal allograft were of an effector memory phenotype. Therefore, these cells have been antigen challenged and are able to rapidly exert immunological responses. Both the CD103+ and CD103− T_{RM} cell subsets had the capacity to produce TNFα, a cytokine involved in, among others, the activation of endothelial cells, thereby attracting other T cells to the site of inflammation[29]. The capacity of the T_{RM} cells to produce IFNγ and the presence of preloaded granzyme B positive granules underlines their cytotoxic phenotype. Low levels of perforin were measured in the T_{RM} cells which is in line with previous studies[30,31]. In these studies, perforin was rapidly upregulated upon antigen stimulation, delineating a dynamic process[30,32]. Here we found that T_{RM} cells present in renal allografts are potentially harmful cells that might contribute to the process of allograft rejection. However, additional experiments need to clarify the exact roles of the T_{RM} cell subsets in the alloimmune response and show causality. For future studies, it would be of interest to include the number of cells per gram tissue. The functional profiles of the T_{RM} subtypes found in the renal allograft were comparable to those found in the T_{RM} subsets residing in the spleen. This supports that we have identified T_{RM} cells in the renal allograft.

Memory T cell signalling is still occurring under immunosuppression because these cells are less reliant on co-stimulatory signals[33–36]. For this reason, we can hypothesize about the long lasting persistence of T_{RM} cells within the renal allograft. Also, the distribution of immunosuppressive agents into the tissue may influence the presence of T_{RM} cells. For instance, alemtuzumab depletes circulating CM T cells in leukemic cutaneous T cell lymphoma patients without completely compromising the immune response to infection, since the skin resident memory cells are spared[37]. The samples analysed in this study are a heterogeneous group with different types of end-stage immunological transplant failure. Further study on the differentiation and function of T_{RM} cells upon

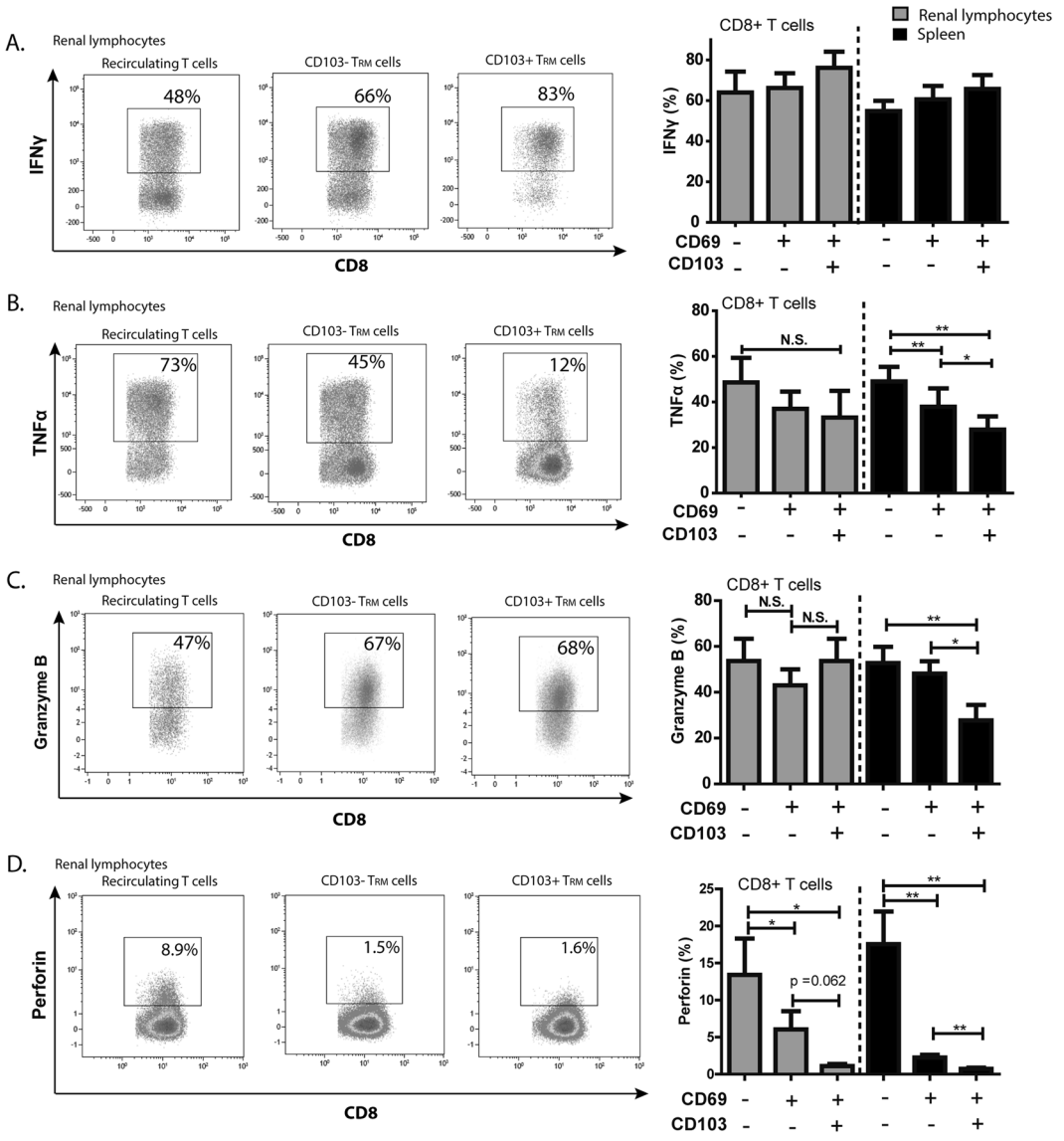

Figure 5. T_{RM} cells are capable of producing effector molecules. (**A**,**B**) Proportions of IFNγ (**A**) and TNFα (**B**) producing cells are depicted upon 4 hours PMA/ionomycin stimulation in the presence of monensin and brefeldin A. Cytokine proportions were measured in renal lymphocytes and splenocytes within the recirculating T cells, CD103− T_{RM} cells, and CD103+ T_{RM} cells of the CD8+ T cell compartment. (**C**,**D**) Frequencies of granzyme B (**C**) and perforin (**D**) levels were measured in the recirculating T cells, CD103− T_{RM}, and CD103+ T_{RM} cells of the CD8+ T cell compartment. Frequencies of positive cells were shown as mean with the SEM (renal lymphocytes $n = 6$, spleen $n = 10$). Significant differences were calculated and depicted (N.S. = not significant, $*p < 0.05$, $**p < 0.01$).

transplantation, would benefit from similar studies on cells harvested from healthy renal tissue or grafts undergoing an evolving rejection, which for obvious reasons is not possible in transplant recipients. The best alternative for healthy renal tissue would be the use of kidneys discarded for transplantation. Our first findings showed the presence of T_{RM} cells in these kidneys with comparable frequencies of CD103− and CD103+ T_{RM} cells as found in the transplant nephrectomies.

The results of our study reveal that donor-derived lymphocytes are replaced by their recipient counterparts within five months after transplantation and that the recipient-derived T cells differentiate locally towards a resident memory phenotype. The rapid presence of recipient T_{RM} cells in these specimens sheds light on the important role of this cell type in the process of alloreactivity. The repopulation by recipient lymphocytes has also been observed in lung and intestinal allografts[38,39]. The prolonged retention of the CD103+ T_{RM} cells compared to the other donor-derived T cells supports that this subtype of T_{RM} cells is highly capable to bind to epithelial cells of the renal allograft (Fig. 6). The retention of donor-derived T_{RM} cells might have a protective role in the renal allograft since irradiation of donor cells in rodent models resulted in rejection of liver transplants[40,41]. Also, in visceral transplant patients, T cell chimerism is observed in the absence of graft-*versus*-host disease

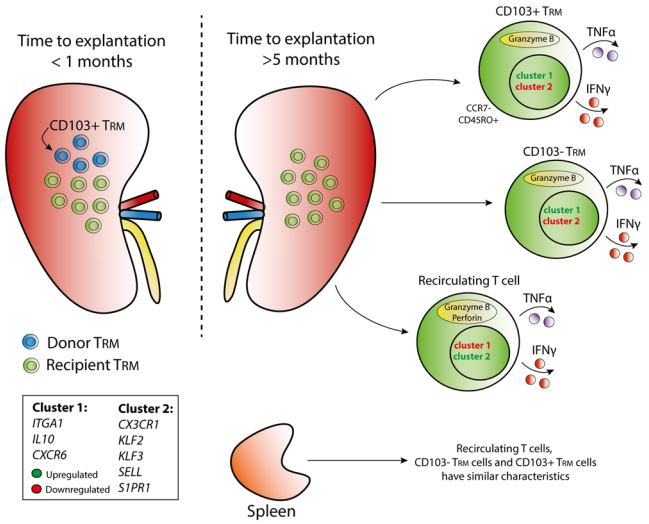

Figure 6. Schematic overview of T_{RM} cell characteristics in the renal allograft. Distribution of donor-derived and recipient-derived tissue-resident memory (T_{RM}) cells and the phenotypic and functional characteristics of the recipient-derived T_{RM} cells in the explanted renal allograft are depicted in a schematic overview. Cluster one and cluster two indicate T_{RM} core genes of which the expression was measured. Cluster one consists of genes involved in T cell activation (*ITGA1*, *IL10*, and *CXCR6*) and cluster two consists of genes involved in T cell migration (*CX3CR1*, *KLF2*, *KLF3*, *SELL*, *S1PR1*).

(GVHD)[21]. Donor-derived cells with graft specific TCR clones are even thought to slow down the constant threat of recipient-derived T cells, illustrating that the balance between graft-*versus*-host (GvH) and host-*versus*-graft (HvG) clones *in situ* influences lymphocyte turnover and development of rejection[22]. A rapid clearance of the donor-derived cells may thus contribute to the rejection of the renal allograft. The low IFNγ-producing response of the renal lymphocytes to recipient PBMCs that we measured might be due to the mixed population of donor and recipient cells within the renal lymphocytes. This observation might be a reflection of the potential GvH response which may also explain a lower response to the donor cells, in line with the findings of Zuber *et al.*[22]. For future experiments, it is of interest to compare the GvH and HvG T cell balance in protocol biopsies at different time points after transplantation and compare this balance between patients with and without rejection. In addition to the response to the allograft, T_{RM} cells also recognize and clear pathogens. Therefore, it is tempting to speculate that the T_{RM} cells are both friends and foes to the renal allograft. Virus-specific T_{RM} cells are known to be able to quickly exert their effector function within the peripheral tissue, and thus the T_{RM} cells present in the renal allograft may also exert this function[20,42]. Therefore, the precise contribution of donor and recipient T_{RM} cells to alloreactivity is of high interest for future studies.

In conclusion, our results demonstrate that T_{RM} cells are present in the human renal allograft and that donor-derived T_{RM} cells are replaced within the first months after transplantation by recipient T_{RM} cells, which have the capacity to aggressively respond to the allograft. Understanding the potentially destructive or protective roles of the T_{RM} cells in the renal allograft is of high interest to enhance renal transplant outcomes.

Materials and Methods

Study population. Thirteen transplant nephrectomy specimens and two kidneys that were discarded for transplantation were studied. The characteristics of the patients from whom the transplant nephrectomies were derived are described in Table 1. Of these nephrectomies, the pathological features corresponding to the type of renal allograft rejection were classified according to the Banff'17 classification[43]. In this study, residual material previously used for histopathological diagnosis was analysed. Residual materials were used in accordance with non-WMO compliant research that is regulated by the Dutch Code of Conduct (Federa). Splenocytes were obtained from deceased organ donors and peripheral blood mononuclear cells (PBMCs) were from healthy controls. The Medical Ethical Committee of the Erasmus MC, University Medical Center, approved this work (MEC-2010-022). All experiments were performed in accordance with relevant guidelines and regulations as described by our institution. All patients gave written informed consent. No organs were procured from (executed) prisoners.

Isolation of lymphocytes. Half of the renal allograft (cortex and medulla) was processed towards a single cell suspension, the other half was used for routine diagnostic assessment. The renal allograft was thoroughly rinsed with PBS to remove peripheral cells and afterwards dissected into small pieces ($<0.5\,cm^3$) and incubated for 60 minutes at 37 °C with 1.1 mg/ml collagenase IV (Serva, Heidelberg, Germany). The collagenase treatment was stopped by the addition of heat-inactivated fetal bovine serum with an end concentration of 10%. The tissue suspension was filtered through different sieves up to a 100 μm sieve (Greiner Bio-One, Kremsmünster, Austria) followed by a Ficoll-Paque Plus procedure (GE healthcare, Uppsala, Sweden). Isolated cells were stored at −190 °C

until further use. Afterwards, cells were thawed and analysed by flow cytometry and reverse transcription-qPCR (RT-qPCR) to determine their phenotype and gene expression profile.

Human splenocytes were disrupted and filtered through a 70 μm cell strainer (Greiner Bio-one, Alphen a/d Rijn, The Netherlands) to obtain a single-cell suspension. Ficoll-paque (Amersham Pharmacia Biotech, Uppsala, Sweden) density gradient was used to collect mononuclear cells. Human PBMCs were isolated with the Ficoll-paque density gradient method.

Flow cytometric and functional analysis. Renal lymphocytes, splenocytes and PBMCs were stained with the following antibodies to characterize the T_{RM} phenotype: CD3 brilliant violet 510 (BV510; Biolegend, San Diego, CA, USA), CD8 Allophycocyanin-Cy7 (APC-Cy7; Biolegend), CD4 fluorescein isothiocyanate (FITC; BD, Franklin Lakes, New Jersey, USA) CD69 brilliant violet 421 (BV421; BD), CD103 phycoerythrin-cyanine7 (PE-Cy7; Biolegend). Viability was measured with the live-dead marker 7-aminoactinomycin (7-AAD; BD). FACS flow enriched with bovine serum albumin was used to wash the cells and block a-specific antibody interactions.

The donor or acceptor origin of the cells was determined with monoclonal antibodies (mAb) directed against human leukocyte antigen (HLA) class I antigens of the donor or acceptor. mAb used are listed in Supplemental Table 1, and were developed at Leiden University Medical Centre. We performed single labelling with either an antigen for which solely the donor was positive or solely the acceptor was positive.

The cytotoxic potential of T_{RM} cells was analysed by measuring intracellular granzyme B and perforin. Cells were stained as described above for T_{RM} cells. Afterwards, the cells were immediately fixed with FACS lysing solution (BD) and permeabilized with PERM II (BD). Subsequently, cells were stained intracellularly with granzyme B Allophycocyanin (APC) (Biolegend) and perforin phycoerythrin (PE; Biolegend).

The cytokine-producing capacity of the cells was measured after the cells were stimulated for four hours with 50 ng/ml phorbol myristate acetate (PMA) and 1 μg/ml ionomycin (Sigma-Aldrich, St. Louis, MO, USA) at 37 °C. Monensin and Brefeldin A (GolgiStop and GolgiPlug, BD Biosciences, Franklin Lakes, NJ, USA) were used to promote intracellular accumulation of the cytokines. PMA/ionomycin stimulation was stopped by adding Ethylene-diamine-tetra-acetic acid. Subsequently, cells were stained with the T_{RM} surface staining mixture and fixed and permeabilized as described above. The following mAb were used to measure cytokine production: interferon-γ (IFNγ) FITC (BD Biosciences), and tumour necrosis factor-α (TNFα) PE (Biolegend). Cell samples were measured on the FACSCanto II (BD) and analysed with Kaluza Analysis 1.5a software (Beckman Coulter, Brea, CA, USA).

Allogeneic reactivity. Mixed lymphocyte reactions (MLR) were performed in order to study T cell-reactivity of the renal lymphocytes following stimulation with donor cells, 3rd party cells, or recipient PBMCs. Renal lymphocytes were thawed and labelled with carboxyfluorescein succinimidyl ester (CFSE; Molecular Probes®, Leiden, The Netherlands). Next, the renal lymphocytes were stimulated at 5×10^4 cells per well with irradiated donor cells, 3rd party cells, or recipient PBMCs (40 Gray) from which the CD3+ T cells had been depleted with magnetic-activated cell sorting (MACS). The cells were cultured at a ratio 1:1 in human culture medium (HCM) and after 7 days the CFSE dilution was measured on the FACSCanto II, indicating the amount of proliferation. Degranulation was measured by APC-labelled anti-CD107a (BD).

IFNγ ELISPOT. The frequencies of IFNγ producing cells upon stimulation with donor cells, 3rd party cells, or recipient PBMCs were measured with an Enzyme-Linked ImmunoSpot (ELISPOT) assay (U-CyTech Biosciences, Utrecht, The Netherlands). Briefly, anti IFNγ coated plates (U-CyTech Biosciences), were seeded with 100,000 renal lymphocytes and 100,000 irradiated donor cells, 3rd party cells or recipient PBMCs. Upon overnight incubation, plates were washed and incubated with biotinylated anti-human IFNγ detection antibody and streptavidin-HRP conjugate followed by the addition of AEC substrate (U-CyTech Biosciences). Spots were analysed using the ELISPOT reader (Bioreader®-600V, BIO-SYS GmbH, Karben, Germany).

Cell sorting of T_{RM} cells and RT-qPCR analysis. To determine the expression levels of a set of T_{RM} key genes of the CD103+ and CD103− T_{RM} cells and CD69−CD103− recirculating T cells, we performed RT-qPCR analysis on FACS-sorted, pure (>95%) T cell populations. Renal lymphocytes and splenocytes were sorted with the BD-FACSAria II SORP™. Subsequently, cells were pelleted and snap frozen and stored at −190 °C until further use.

RNA was isolated with the RNeasy Micro Kit (Qiagen, Hilden, Germany) for the collection of high-quality RNA. Total RNA was subsequently reverse transcribed with oligo-dT. We used RT-qPCR to quantify the amount of *ITGA1*, *IL10*, *CXCR6*, *CX3CR1*, *KLF2*, *KLF3*, *SELL*, *S1PR1*, and the housekeeping gene *glyceraldehyde 3-phosphate dehydrogenase* (*GAPDH*). Assay-on-demand products for the detection and quantification of the different genes were used and are listed in Supplemental Table 2 (ThermoFisher, Waltham, MA, USA). The amount of each target gene was quantified by measuring the threshold cycle (Ct), which was transformed on a TaqMan Real-Time PCR system to the number of cDNA copies ($2^{(40\text{-}Ct)}$). The relative concentrations of the analysed genes were normalized to the relative concentration of the housekeeping gene GAPDH present in each sample. Heatmapper software was used to cluster the cell-sorted samples based on the expression of the above described genes[44].

Statistical analysis. Statistical analyses were performed using GraphPad Prism 5 software (GraphPad Software; San Diego, CA, USA). Differences between paired groups were analysed with the Wilcoxon signed-rank test. A two-tailed p-value of < 0.05 was considered statistically significant.

Data Availability

All data generated or analysed during this study are included in this published article and the Supplementary Information File.

References

1. Masopust, D., Vezys, V., Marzo, A. L. & Lefrancois, L. Preferential localization of effector memory cells in nonlymphoid tissue. *Science* **291**, 2413–2417 (2001).
2. Park, C. O. & Kupper, T. S. The emerging role of resident memory T cells in protective immunity and inflammatory disease. *Nat Med* **21**, 688–697 (2015).
3. Woon, H. G. *et al*. Compartmentalization of Total and Virus-Specific Tissue-Resident Memory CD8+ T Cells in Human Lymphoid Organs. *PLoS Pathog* **12**, e1005799 (2016).
4. Watanabe, R. *et al*. Human skin is protected by four functionally and phenotypically discrete populations of resident and recirculating memory T cells. *Sci Transl Med* **7**, 279ra239 (2015).
5. Wakim, L. M., Woodward-Davis, A. & Bevan, M. J. Memory T cells persisting within the brain after local infection show functional adaptations to their tissue of residence. *Proc Natl Acad Sci USA* **107**, 17872–17879 (2010).
6. Thome, J. J. *et al*. Spatial map of human T cell compartmentalization and maintenance over decades of life. *Cell* **159**, 814–828 (2014).
7. Mackay, L. K. *et al*. Cutting edge: CD69 interference with sphingosine-1-phosphate receptor function regulates peripheral T cell retention. *J Immunol* **194**, 2059–2063 (2015).
8. Pham, T. H., Okada, T., Matloubian, M., Lo, C. G. & Cyster, J. G. S1P1 receptor signaling overrides retention mediated by G alpha i-coupled receptors to promote T cell egress. *Immunity* **28**, 122–133 (2008).
9. Shiow, L. R. *et al*. CD69 acts downstream of interferon-alpha/beta to inhibit S1P1 and lymphocyte egress from lymphoid organs. *Nature* **440**, 540–544 (2006).
10. Kumar, B. V. *et al*. Human Tissue-Resident Memory T Cells Are Defined by Core Transcriptional and Functional Signatures in Lymphoid and Mucosal Sites. *Cell Rep* **20**, 2921–2934 (2017).
11. Cepek, K. L., Parker, C. M., Madara, J. L. & Brenner, M. B. Integrin alpha E beta 7 mediates adhesion of T lymphocytes to epithelial cells. *J Immunol* **150**, 3459–3470 (1993).
12. Pallett, L. J. *et al*. IL-2(high) tissue-resident T cells in the human liver: Sentinels for hepatotropic infection. *J Exp Med* **214**, 1567–1580 (2017).
13. Sathaliyawala, T. *et al*. Distribution and compartmentalization of human circulating and tissue-resident memory T cell subsets. *Immunity* **38**, 187–197 (2013).
14. Purwar, R. *et al*. Resident memory T cells (T(RM)) are abundant in human lung: diversity, function, and antigen specificity. *PLoS One* **6**, e16245 (2011).
15. Hombrink, P. *et al*. Programs for the persistence, vigilance and control of human CD8(+) lung-resident memory T cells. *Nat Immunol* **17**, 1467–1478 (2016).
16. Stelma, F. *et al*. Human intrahepatic CD69+CD8+ T cells have a tissue resident memory T cell phenotype with reduced cytolytic capacity. *Sci Rep* **7**, 6172 (2017).
17. Steinert, E. M. *et al*. Quantifying Memory CD8 T Cells Reveals Regionalization of Immunosurveillance. *Cell* **161**, 737–749 (2015).
18. Ma, C., Mishra, S., Demel, E. L., Liu, Y. & Zhang, N. TGF-beta Controls the Formation of Kidney-Resident T Cells via Promoting Effector T Cell Extravasation. *J Immunol* **198**, 749–756 (2017).
19. Prosser, A. C., Kallies, A. & Lucas, M. Tissue-Resident Lymphocytes in Solid Organ Transplantation: Innocent Passengers or the Key to Organ Transplant Survival? *Transplantation* **102**, 378–386 (2018).
20. Park, S. L. *et al*. Local proliferation maintains a stable pool of tissue-resident memory T cells after antiviral recall responses. *Nat Immunol* **19**, 183–191 (2018).
21. Zuber, J. *et al*. Macrochimerism in Intestinal Transplantation: Association With Lower Rejection Rates and Multivisceral Transplants, Without GVHD. *Am J Transplant* **15**, 2691–2703 (2015).
22. Zuber, J. *et al*. Bidirectional intragraft alloreactivity drives the repopulation of human intestinal allografts and correlates with clinical outcome. *Sci Immunol* **1** (2016).
23. Beura, L. K., Rosato, P. C. & Masopust, D. Implications of Resident Memory T Cells for Transplantation. *Am J Transplant* **17**, 1167–1175 (2017).
24. Hadley, G. A. *et al*. CD103+ CTL accumulate within the graft epithelium during clinical renal allograft rejection. *Transplantation* **72**, 1548–1555 (2001).
25. Robertson, H., Wong, W. K., Talbot, D., Burt, A. D. & Kirby, J. A. Tubulitis after renal transplantation: demonstration of an association between CD103+ T cells, transforming growth factor beta1 expression and rejection grade. *Transplantation* **71**, 306–313 (2001).
26. Wang, D. *et al*. Regulation of CD103 expression by CD8+ T cells responding to renal allografts. *J Immunol* **172**, 214–221 (2004).
27. Yuan, R. *et al*. Critical role for CD103+CD8+ effectors in promoting tubular injury following allogeneic renal transplantation. *J Immunol* **175**, 2868–2879 (2005).
28. Ding, R. *et al*. CD103 mRNA levels in urinary cells predict acute rejection of renal allografts. *Transplantation* **75**, 1307–1312 (2003).
29. Agius, E. *et al*. Decreased TNF-alpha synthesis by macrophages restricts cutaneous immunosurveillance by memory CD4+ T cells during aging. *J Exp Med* **206**, 1929–1940 (2009).
30. Piet, B. *et al*. CD8(+) T cells with an intraepithelial phenotype upregulate cytotoxic function upon influenza infection in human lung. *J Clin Invest* **121**, 2254–2263 (2011).
31. Seidel, J. A. *et al*. Skin resident memory CD8(+) T cells are phenotypically and functionally distinct from circulating populations and lack immediate cytotoxic function. *Clin Exp Immunol* (2018).
32. Voskoboinik, I., Whisstock, J. C. & Trapani, J. A. Perforin and granzymes: function, dysfunction and human pathology. *Nat Rev Immunol* **15**, 388–400 (2015).
33. Zhai, Y., Meng, L., Gao, F., Busuttil, R. W. & Kupiec-Weglinski, J. W. Allograft rejection by primed/memory CD8+ T cells is CD154 blockade resistant: therapeutic implications for sensitized transplant recipients. *J Immunol* **169**, 4667–4673 (2002).
34. Valujskikh, A., Pantenburg, B. & Heeger, P. S. Primed allospecific T cells prevent the effects of costimulatory blockade on prolonged cardiac allograft survival in mice. *Am J Transplant* **2**, 501–509 (2002).
35. de Leur, K. *et al*. Characterization of ectopic lymphoid structures in different types of acute renal allograft rejection. *Clin Exp Immunol* **192**, 224–232 (2018).
36. Kannegieter, N. M. *et al*. Differential T Cell Signaling Pathway Activation by Tacrolimus and Belatacept after Kidney Transplantation: Post Hoc Analysis of a Randomised-Controlled Trial. *Sci Rep* **7**, 15135 (2017).
37. Clark, R. A. *et al*. Skin effector memory T cells do not recirculate and provide immune protection in alemtuzumab-treated CTCL patients. *Sci Transl Med* **4**, 117ra117 (2012).
38. Bittmann, I. *et al*. Cellular chimerism of the lung after transplantation. An interphase cytogenetic study. *Am J Clin Pathol* **115**, 525–533 (2001).
39. Iwaki, Y. *et al*. Replacement of donor lymphoid tissue in small-bowel transplants. *Lancet* **337**, 818–819 (1991).
40. Zhang, Y. *et al*. Total body irradiation of donors can alter the course of tolerance and induce acute rejection in a spontaneous tolerance rat liver transplantation model. *Sci China Life Sci* **55**, 774–781 (2012).
41. Sun, J., McCaughan, G. W., Gallagher, N. D., Sheil, A. G. & Bishop, G. A. Deletion of spontaneous rat liver allograft acceptance by donor irradiation. *Transplantation* **60**, 233–236 (1995).
42. Wakim, L. M., Waithman, J., van Rooijen, N., Heath, W. R. & Carbone, F. R. Dendritic cell-induced memory T cell activation in nonlymphoid tissues. *Science* **319**, 198–202 (2008).

43. Haas, M. *et al*. The Banff 2017 Kidney Meeting Report: Revised diagnostic criteria for chronic active T cell-mediated rejection, antibody-mediated rejection, and prospects for integrative endpoints for next-generation clinical trials. . *Am J Transplant* **18**, 293–307 (2018).
44. Babicki, S. *et al*. Heatmapper: web-enabled heat mapping for all. *Nucleic Acids Res* **44**, W147–153 (2016).

Acknowledgements

We would like to thank D. Reijerkerk for the technical assistance with the IFNγ ELISPOT assay and M. van der Zwan for helping us with the collection of the clinical data. This work was supported by a grant from the Erasmus MC, University Medical Centre, Rotterdam, awarded by the Erasmus MC Medical research advisory committee (Mrace), Grant No. 343564.

Author Contributions

K.L. participated in research design, performing the research, data analysis and writing of the article; M.D., G.G. and A.P. participated in performing the research, data analysis and revision of the article; D.H. participated in research design and revision of the article; O.C. and M.C. participated in performing the research and revision of the article; F.C. and A.M. provided analytical tools and participated in revision of the article; H.K. and F.D. participated in collecting study material and participated in revision of the article; L.L. and R.H. participated in research design and revision of the article; C.B. participated in research design and writing of the article.

Additional Information

Supplementary information accompanies this paper at https://doi.org/10.1038/s41598-019-42401-9.

Competing Interests: D.A. Hesselink has received lecture and consulting fees from Astellas Pharma and Chiesi Farmaceutici SpA, as well as grant support from Astellas Pharma, Bristol-Myers Squibb, and Chiesi Farmaceutici SpA (paid to the Erasmus MC). F.J.M.F. Dor has received lecture and consulting fees from Astellas Pharma, Chiesi Farmaceutici SpA, Sandoz, and TEVA pharmaceuticals.

Publisher's note: Springer Nature remains neutral with regard to jurisdictional claims in published maps and institutional affiliations.